Digital Image Correlation (DIC) and Finite Element Modelling(FEM) Assessment on Hybrid Composite Carbon Glass Fibre under Tensile and Flexural Loading

Ahmad Fuad Ab Ghani[1*], Ridhwan Jumaidin[1],Mohamed Saiful Firdaus Hussin[1],Sivakumar Dharmalingam[2], Fudhail Abdul Munir[2], Rahifa Ranom[3] and Jamaluddin Mahmud[4]
[1]Faculty of Engineering Technology Mechanical and Manufacturing
[2]Faculty of Mechanical Engineering, [3]Faculty of Electrical Engineering
Universiti Teknikal Malaysia Melaka (UTeM), Hang Tuah Jaya,76100, Melaka, Malaysia
[4]Faculty of Mechanical Engineering, Universiti Teknologi MARA (UiTM), 40450,Shah Alam, Selangor, Malaysia

***Abstract*— Digital Image Correlation results of in plane strain measurement is discussed and synthesized on deviation obtained from Finite Element Modelling strain contour. In plane deformation measurement technique of Digital Image Correlation (DIC) full field deformation on Hybrid Composite C/GFRP with comparison with Finite Element Modelling (FEM).The deformation displacement, in-plane strain *xx*, in-plane strain *yy* and in-plane shear strain *xy* are extracted from strain gauge and digital image correlation (DIC) technique via high-speed camera that captures during the experiment.Proposing the in plane deformation measurement technique of Digital Image Correlation (DIC) on Hybrid Composite C/GFRP with comparison to Finite Element Modelling (FEM) via Median Value**

***Index Term*— Digital Image Correlation, Hybrid Composite, CFRP,GFRP, FEM Composite**

I. Introduction

It has been proved that incorporation of GF into CF is possible with a view to improve the failure strain of CFRP, turning the materials to a combination system called hybrids [1],[2]. Apart from the toughness issue, CF are also very expensive which is regarded as the main drawback why CFRP are only popular in aero industries and automotive sector where weight saving is considered to be the primary concern [2]. GF are cheaper than CF and the glass fibre reinforced polymers (GFRP) have been increasingly utilized to substitute steel in automotive industry. Hybridization of GF into CF selectively could be an effective means to reduce vehicle weight without implying high cost [3].Although the innovative fibre hybridization has been around for quite some time [4][5], recent frontier of new materials creates new and exciting possibilities for obtaining superior hybrid composites tailored for particular applications. In order to achieve both design adaptability and reduction of cost, there is a need to develop the carbon/glass hybrid composite and evaluate their mechanical properties.Recently, the development of robust, fast and affordable tools for full-field kinematic measurements prompts more and more experimentalists to utilize such techniques. Digital image correlation methods (DIC) first been developed in the early 1980s has influenced positively in the field of mechanics of solids and structures and it is still experiencing interesting developments [6][7][8]. The idea is to measure the displacement fields of surfaces of stressed specimens and structures from images acquired at different stages of loading. A specific advantage of this tool is that it exploits numerical images that usually acquired by optical means. More generally, full-field measurements constitute an opportunity to bridge the gap between experiments and simulations allowing for direct displacement and strain comparisons [7],[9],[10]. It is still in infancy stage of research on full field in-plane deformation of Hybrid C/GFRP. The full field offers improved measurement on deformation of Hybrid C/GFRP. The computation using full field measurement technique such as DIC provides alternative to conventional strain method and DIC able to offer new findings from strain measurement of in-plane hybrid composite.

A. Digital Image Correlation (DIC) on Composite Material Characterization

Significant advancements have been seen in recent years among researchers in developing new experimental Digital Image Correlation (DIC) methods and post-processing such as image processing and enhancement in the computational algorithms. DIC is a non-contact, optical method which captures digital images of a surface of an object then performs

Correspoding author, Dr Ahmad Fuad Ab Ghani is a senior lecturer at Faculty of Engineering Technology Mechanical and Manufacturing, Universiti Teknikal Malaysia Melaka. Author can be contacted at ahmadfuad@utem.edu.my.

the image analysis to obtain full-field deformation and measurements. This can be achieved by creating different methods like dots, grids and lines among others on the specimen surface. This technique starts with a reference image (before loading) followed by a series of pictures taken during the deformation. Blaber *et al.* [11] formulated a new free DIC open source software package Ncorr. Ncorr is an open source subset based on the 2D DIC software that incorporates DIC algorithms discussed in the literature with post-processing capability. Deformed images show a different dot pattern relative to the initial non-deformed reference image. These patterns difference can be calculated by performing correlation of the pixels of the reference image and any deformed image, and a full-field displacement measurement can be computed. The strain distribution can then be obtained by applying the derivatives in the displacement field. To apply this method, the object under study needs to be prepared with random dot pattern speckle pattern to its surface [12]. Reference picture is segmented into smaller zones called subsets. The deformation recorded in DIC system is expected to be homogeneous from each subset, and the deformed subsets with speckle pattern are traced in the current image as illustrated in Figure 1. The illustration shows the sequence of searching initial guess and correlation [11].

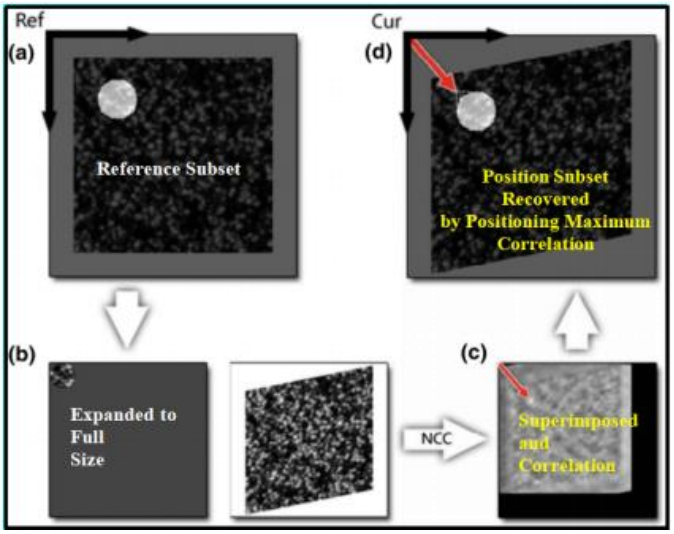

Fig. 1. Illustration Shows Sequence of Searching Initial Guess and Correlation [10]

Siddiqui *et al.* [13] computed the longitudinal and measurement of lateral strains in an uniaxial test. The strains computed using the DIC method were then compared with strain gauges and extensometer for validation of strain measurement. The measured values of the Poisson ratio obtained for aluminium and steel specimens are quite close to the ones measured with strain gauges and reported in the literature. Moreover, it was also reported that the the Poisson ratio of composite specimens where the DIC technique was employed recorded similar readings to that of the strain gauge. For surface deformation computation utilizing 2D Digital Image Correlation (DIC) technique, emphasis should be given on the positioning of the specimen under testing, light intensity and sources as well as the camera lens and its capability/resolution/frame rate of the camera. Accurate measurement relies heavily on imaging system configuration. In principle, a sample with random speckle pattern sprayed on the surface must be positioned perpendicular to the camera to avoid any out of plane motion. After the entire load applied events, a series of images are taken before and after loading and deformation and finally stored in the computer for post-processing images to obtain displacement contour/field using DIC algorithm as shown in Figure 2. Basically from a technical perspective, for 2D DIC, image resolution plays a vital role in measurement accuracy [14].

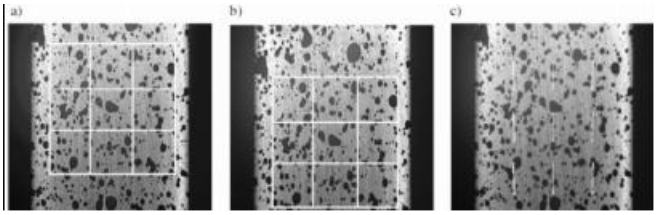

Fig. 2. Computation of The Displacement Vectors Using The Digital Image Correlation:a) Reference Image; b) Deformed Subset/Image; c) Displacement Field [14]

To achieve an effective correlation, the speckle pattern must be of high contrast and non-repetitive. The large pattern can bring several subsets to track only entirely on the black field or neither entirely on a white field. If the pattern is too small, it may cause the inability of the resolution of the camera to precisely identify the specimen in terms of information extraction [15]. The accuracy of the measurement in DIC also can be affected by subset size and subset shape function. Larger size of subsets also can lead into larger error in the approximation of the underlying deformations. Larger size of subset can produce problem in matching the shape of speckle pattern before and after deformation. However, when the subset is too small it produces inadequate enough information of speckle to correlate [15]. In another research, tests were conducted using Universal Testing Machine, and the load was applied under displacement control mode until tensile rupture of the coupon [16]. Both CivEng Vision and *Ncorr* software programs were used to process the digital images taken at 5 seconds time interval with the aim of computing the displacements. The DIC technique was used for extracting damage pattern information, namely the crack number, location, and width, and recording evolution during the test. The combination between the strain gauges and DIC methods allow for the enhancement of the identification of the mechanical properties of the [16]. There was reported literature on Digital Image Correlation (DIC) on bending specimen of conventional composite material in computing deflection but not for transverse strain, ε_{xx} (through thickness plane) and comparison with FEM contour for Hybrid Composite C/GFRP. Apart from that, little research is observed on the study of in-plane longitudinal strain, ε_{yy} comparison between DIC and FEM computation for tensile coupon Hybrid Composite, C/GFRP.

II. METHODOLOGY

The simulation is performed systematically to study the deformation according to loading types (tensile and flexural). FE analysis inbuilt composite features in Abaqus 6.14 (2016) material parameter and properties are utilized. The strain contours from simulations are compared to strain contour obtained from DIC post-processing output. For flexural behaviour, through thickness transverse strain, Ɛxx obtained from DIC is compared with FEM simulation together with the deflection computation. The trend of maximum and minimum value of strain computed for tensile loading coupon obtained from Digital Image Correlation (DIC) and Finite Element Modelling (FEM) is then synthesised. A similar approach is also taken on flexural specimens where deflection computed via DIC software is compared with the one simulated in FEM. The transverse strain Ɛxx computed from DIC which is full field deformation is of beneficial tool to predict failure of hybrid composite C/GFRP based on maximum strain criteria, and this is also benchmarked with strain contour produced by FEM simulation.

A Digital Image Correlation

Figure 3 shows the setting up of DIC system to acquire images data from tensile test coupon performed in Static Lab, Faculty of Mechanical Engineering, Universiti Teknikal Malaysia Melaka (UTeM). Deformation displacement, in plane strain xx, in plane strain yy and in plane shear strain xy are extracted from digital image correlation technique using high-speed camera that captures during experiment. High- speed camera used for DIC for this research contain the sensor recording speeds of up to 200,000fps and 800 x 600 resolutions at 1000fps, Camera Display Unit (CDU)[Figure 4] built in measurement, and storage and editing capability. Olympus *i-Speed 2* camera is used to capture images for tensile and bending test. The camera is positioned perpendicular to the specimen under testing. Speckle pattern must be sprayed onto the surface of the coupon [Figure 5].

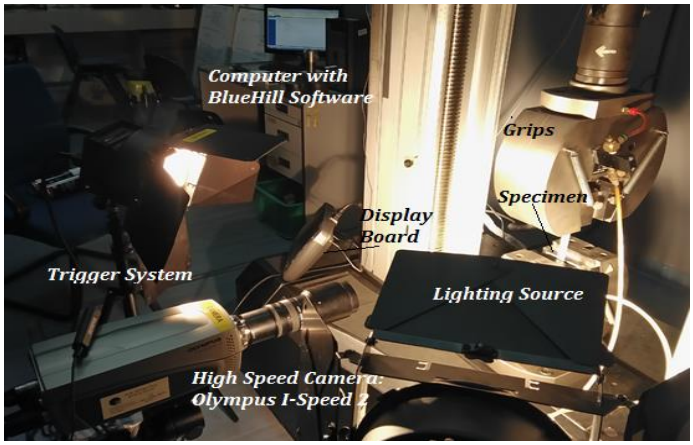

Fig. 3. Setting Up of DIC on Tensile Test Specimen Under Study (CFRP, GFRP and Hybrid Composites CFRP/GFRP)

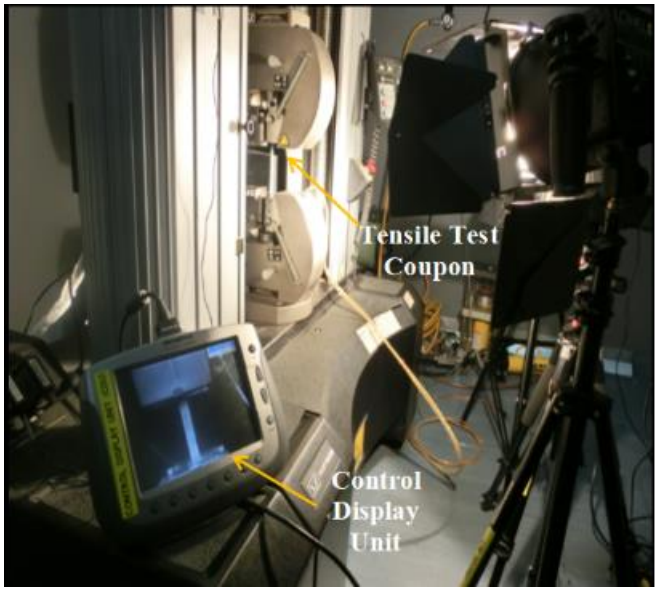

Fig. 4. DIC Setting Up with Display Board to Assist Visualization of Deformation

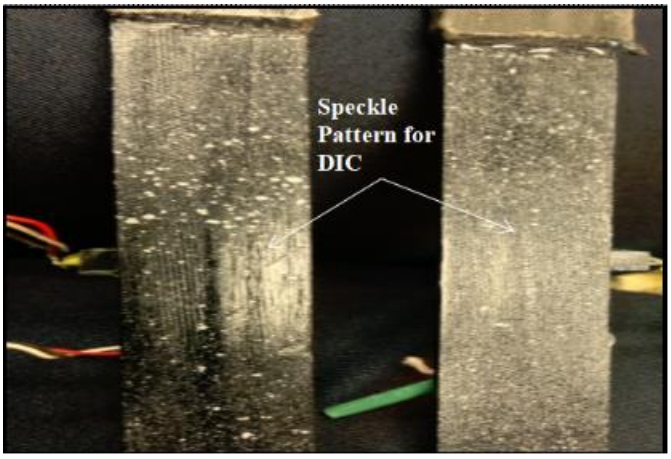

Fig. 5. Black and White Speckle Pattern for DIC Processing of Displacement/Strain

It is expected that this study provides novel insight on the deviation and pattern between full field measurements of in plane strain from DIC with finite element modelling (FEM). This encompass the assessment of tensile test in plane strain, ε_{yy} (longitudinal direction) as well as flexural test (three-point bending) deflection and transverse strain, ε_{xx} at through thickness plane.

B Region of Interest

Figure 6 shows the different between large ROI and small ROI for sample of Hybrid Cross#1. For the small ROI the subset spacing is 6 and the strain radius is 15. Meanwhile, the large ROI subset spacing is 5 and the strain radius is 40. The value of strain for both ROI is a little bit different. The maximum strain for the large ROI is 0.0182 and for small ROI is 0.0186. The median is 0.0143 for small ROI and 0.0145 for large ROI. The

different for value of strains computed accounts for approximately 0.002.

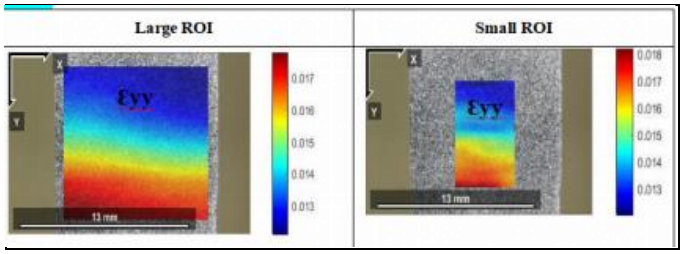

Fig. 6. Effect of Different ROI Size on Strain Computation

The combination method of strain gauges and DIC allows enhancement of identifications for mechanical properties of composite in testing and contributes to a deeper understanding of deformation and development of optimized systems. Subset size of 64 X 64 pixels with image resolution of 250 pixels/mm with LED flash light were used in this DIC set up.

C. Comparison of Strain Contour Computed by DIC and Finite Element Modelling

It is expected that this study provides novel insight on the deviation and pattern between full field measurements of in plane strain from DIC with finite element modelling (FEM). This encompass the assessment of tensile test in plane strain, ε_{yy} (longitudinal direction) as well as flexural test (three-point bending) deflection and transverse strain, ε_{xx} at through thickness plane. This study also highlights the comparison between the DIC displacement as well as the strain contour and measurement obtained through Finite Element Modelling which is numerical in principle.

D. Material Properties of Composite Layups

Composite coupon is modelled base on this Standard Test Methods for tensile test as described in Figure 7 as accordance to ASTM D3039. Material properties for CFRP and GFRP for real scale modelling are tabulated as per Table I.

TABLE I
MATERIAL PROPERTIES FOR CFRP AND GFRP IN FEM

Material Properties	CFRP	GFRP
Longitudinal Tensile Modulus (E_{11}) (MPa)	123989	38137
Transverse Tensile Modulus(E_{22}) (Tensile)(MPa)	7637	9904
Longitudinal Tensile Strength (MPa)	1260	866
Transverse Tensile Strength (MPa)	34.1	62.9
Shear Modulus (GPa)	4.25	3.93
Shear Strength (MPa)	107	121
Longitudinal Compressive Modulus(E_{11}) (MPa)	126200	53900
Transverse Compressive Modulus (GPa)	10.1	14.1

E. Boundary Conditions for Tensile and Three Point Bending (Flexural) Macroscale

Boundary conditions for tensile and flexural loading (three point bending) are set as per experimental set up. For tensile loading, one side being pulled (either by pressure loading or displacement/velocity loading) and another side is pinned/clamped in real case as shown in Figure 3.9.

Fig 7 Displacement Control and Encastre/Fixed Boundary Conditions Under Tensile Loading

Figure 8 depicts the boundary conditions involved in finite element modelling of three-point bending (flexural) which simulate real case at Universal Testing Machine. Pinned support at left and right side of the rollers were modelled which allow rotation to occur. Line load was applied (load controlled) across the mid section of composite plate which undergone compression mode as per Universal Testing Machine. Type of element for composite ply used was S4R, while number of nodes involved was 3553 and number of elements was 3348. For hybrid composites C/GFRP, the maximum stress may not always occur at the outermost layer and depends on the layup scheme and orientation. Stress and strain profile differ on each ply of specimen layup, namely on integration points through the thickness of specimen layup.

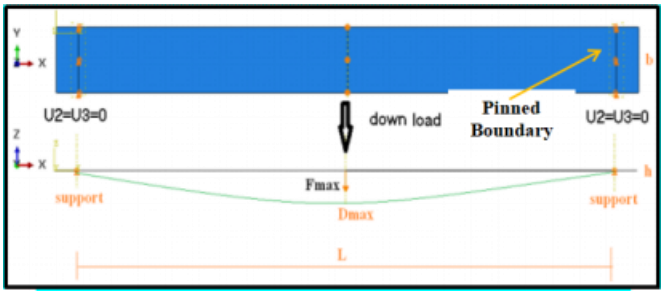

Fig. 8. Boundary Conditions for Three-Point Bending Under Flexural

III. RESULTS AND DISCUSSION

A. *Deformation Comparison of Digital Image Correlation (DIC) on Hybrid Composites C/GFRP Tensile Test with Finite Element Modelling*

Several hybrid composites, namely Hybrid #R, Hybrid #S, Hybrid #Q, Hybrid #P and CFRP 0º under tensile test have been selected with the aim of contour longitudinal strain ε_{yy}, comparison between finite element modelling (FEM) and Digital Image Correlation (DIC) full field strain, ε_{yy}. Figure 9, Figure 10, Figure 11, Figure 12, Figure 13 and Figure 14 illustrate a selected comparison of tensile test coupon digital image correlation ε_{yy} measurement comparison with FEM at 1000N, 2000N and 4000N tensile loading for Hybrid Composite #R. For example, Figure 9 depicts contour of strain, ε_{yy} with Max of 0.0028; Median of 0.0017 and Min of 0.0005.

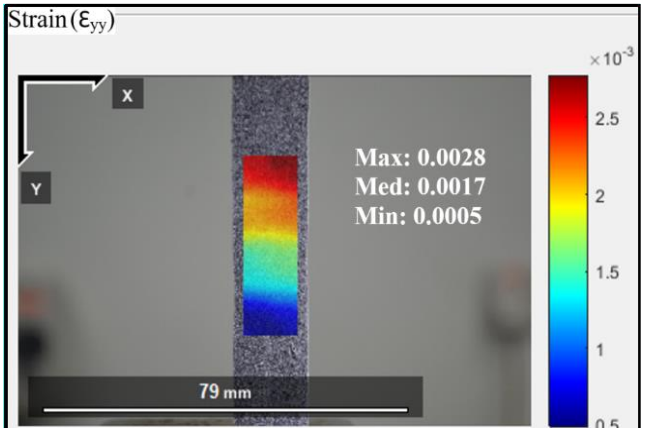

Fig. 9. Contour of Strain yy (ε_{yy}) for Hybrid Composite # R at 1000N Using DIC

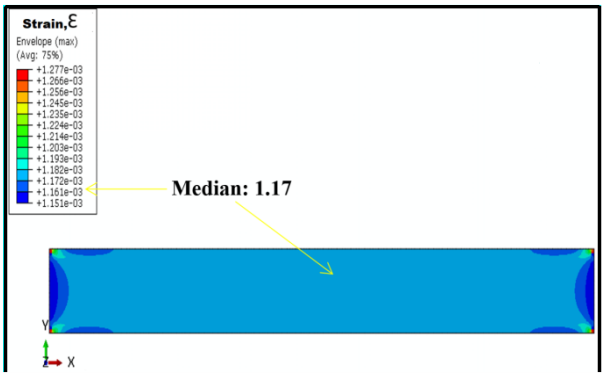

Fig 10 Contour of Strain for Hybrid Composite # R at 1000N Using FEM

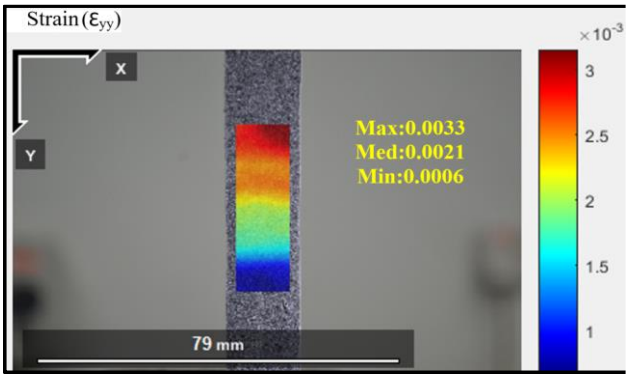

Fig. 11. Contour of Strain yy (ε_{yy}) for Hybrid Composite # R at 3000N Using DIC

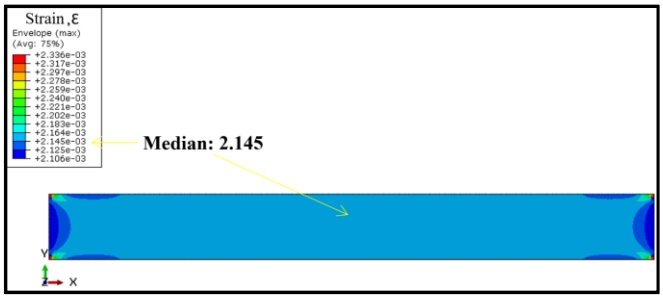

Fig. 12. Contour of Strain,ε for Hybrid Composite # R at 3000N Using FEM

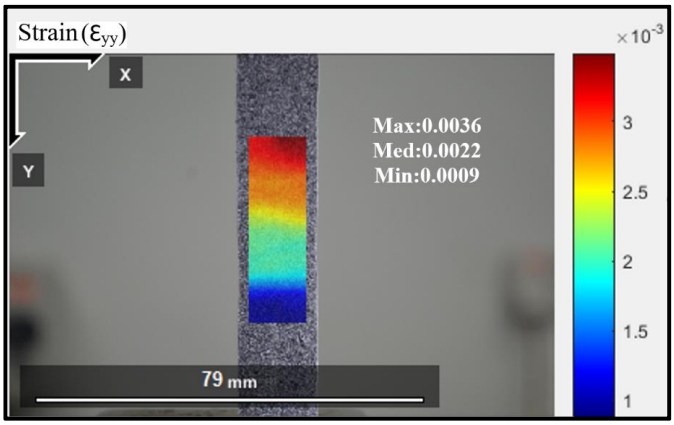

Fig. 13. Contour of Strain yy (ε_{yy}) for Hybrid Composite # R at 4000N Using DIC

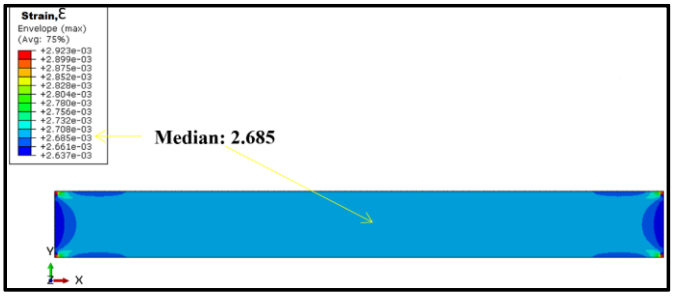

Fig. 14. Contour of Strain yy (εyy) for Hybrid Composite # R at 4000N Using FEM

Summary of deviation between the computation obtained from DIC and FEM with respect to median value of ε_{yy} was plotted as in Figure 15, Figure 16, Figure 17, Figure 18 and Figure 19 for Hybrid #P, Hybrid #Q, Hybrid #R, Hybrid #S

and CFRP 0° respectively. It is observed that the difference of strain between the two methods for CFRP 0° is minimal. The hybrid composites C/GFRP composition produces a significant difference of effect in terms of the deviation, where for most of the exterior layer of CFRP hybrid composites such as Hybrid #P, Hybrid #Q and Hybrid #R, shows a slightly higher deviation of median strain computed. Comparatively, Hybrid #S which comprises of exterior GFRP layup sandwiching CFRP layups exhibits a smaller deviation. Hybrid #P shows the lowest total deviations among the three hybrid composites with exterior CFRP and interior GFRP (Hybrid #P, Hybrid #Q and Hybrid#R). This is due to the fact that the middle CFRP layer acted as a mediator in stress sharing mechanism during load bearing. Incremental composition of GFRP layers between Hybrid #R and Hybrid #Q does also contributed to strain computation deviation between DIC and FEM where Hybrid #R recorded slightly higher values of strain computation.

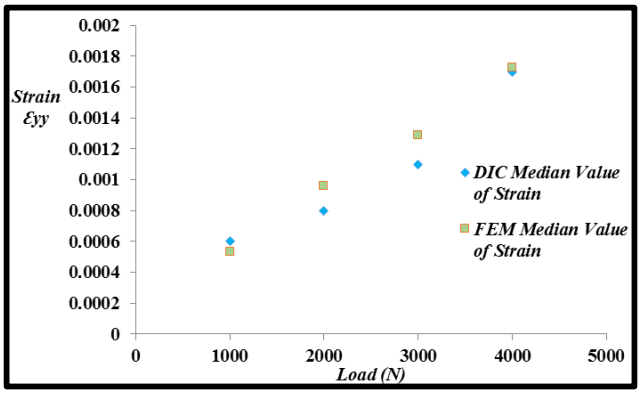

Fig. 15. Deviation of Longitudinal Strain, ε_{yy} Computed Under Tensile Loading for Hybrid#P $[0^{o}_{C}/0^{o}_{2G}/0^{o}_{C}/0^{o}_{2G}/0^{o}_{C}]_{T}$

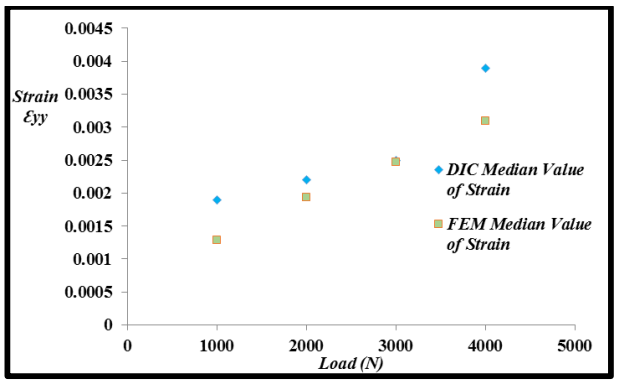

Fig. 16. Deviation of Longitudinal Strain, ε_{yy} Computed Under Tensile Loading for Hybrid#Q $[0^{o}_{C}/0^{o}_{3G}/0^{o}_{C}]_{T}$

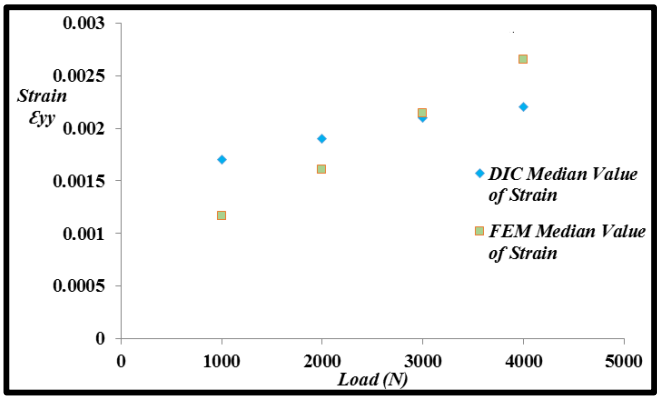

Fig. 17. Deviation of Longitudinal Strain, ε_{yy} Computed Under Tensile Loading for Hybrid#R $[0^{o}_{C}/0^{o}_{6G}/0^{o}_{C}]_{T}$

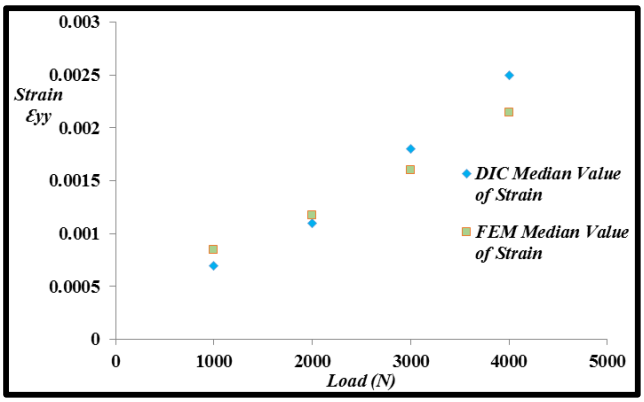

Fig. 18. Deviation of Longitudinal Strain, ε_{yy} Computed Under Tensile Loading for Hybrid#S $[0^{o}_{3G}/0^{o}_{2C}/0^{o}_{3G}]_{T}$

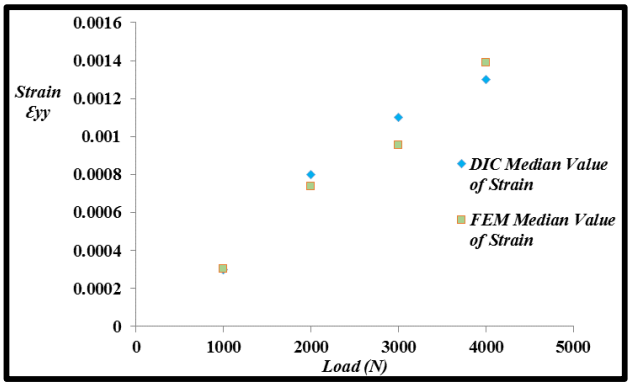

Fig. 19. Deviation of Longitudinal Strain, ε_{yy} Computed Under Tensile Loading for CFRP 0^{o} $[0^{o}_{3C}]_{T}$

B. Flexural Loading Deformation Computation of Hybrid Composite C/GFRP using Digital Image Correlation (DIC) and Finite Element Modelling.

Deflection and displacement for bending test was also successfully measured with the use of DIC which provided accurate in-plane measurement as compared to conventional readings from the Universal Testing Machine deflection display. The value of flexural modulus was also located in between the values of Flexural Modulus CFRP and GFRP again as a result of hybridization. An attempt is made to compare the transverse strain, ε_{xx} at middle section (through thickness in-plane) of the hybrid composite plate under three-point bending with finite element modelling contour. When a homogeneous

elastic material is tested in flexure as a simple beam supported at two points and loaded at the midpoint, the maximum stress in the outer surface of the test specimen occurs at the midpoint as shown in Figure 20. Meanwhile, Figure 21 shows the stress profile extracted at through thickness section of the bending coupon where interior region experiencing compression and exterior region subjected to tensile mode. Top layer be in compress state (negative stress) and bottom layer be in tensile state (positive stress).

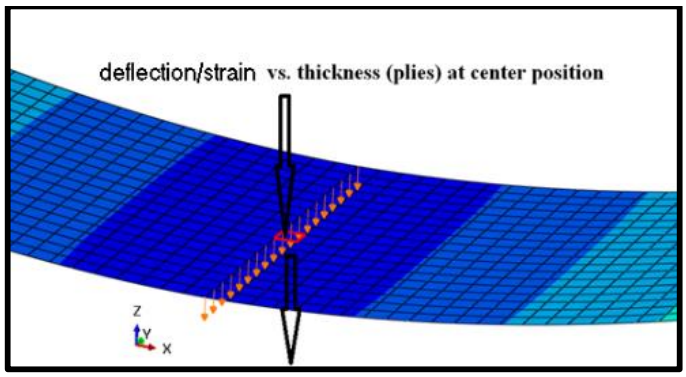

Fig. 20. Region of Applied Line Load, Deflection and Strain Data Extracted at Through Thickness

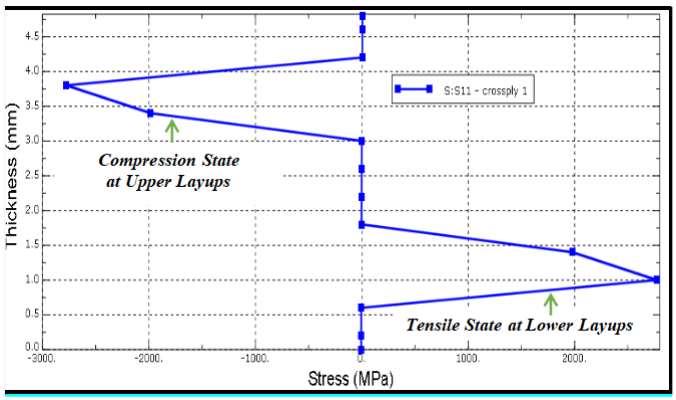

Fig. 21. Stress Profile at Through Thickness of Mid Section of Composite Plate Under Flexural

Selected Hybrid Composites under study for this purpose are Hybrid #D, Hybrid W, Hybrid#P, Hybrid #Q, and Hybrid #R. This achievement opens a huge opportunity for future study on failure prediction of composites and hybrid composites. It can also include other in-plane strain such as through thickness longitudinal strain, ε_{yy} and shear strain, ε_{xy} also profile of deflection for each layup of composite and hybrid composite. Figure 22 and Figure 23 displays comparison of deflection contour for Hybrid #R under three-point bending using DIC and simulation via FEM respectively. Figure 26 and Figure 27 respectively represent the comparisons of deflection contours for Hybrid #D using DIC and simulation via FEM.

A comparison of the transverse strain, ε_{xx} of Hybrid #D, Hybrid #W, Hybrid #P, Hybrid #Q and Hybrid #R between those obtained from DIC and FEM were also performed. The corresponding value of 200N was chosen for all the cases and mid section of through thickness had been selected for region of measurement. Figure 24 and Figure 25 depict the comparison of tranverse strain, ε_{xx} for Hybrid #R between DIC and simulation via FEM at the region of centre of composite plate under three-point bending. Meanwhile Figure 28 and Figure 29 show the assessments of transverse strain, ε_{xx} of Hybrid #D using DIC and simulation of FEM. Due to imperfect geometry mapping there exist local deviations between data that affect the accuracy of the true deviation of results. indicating a non-uniform load distribution.

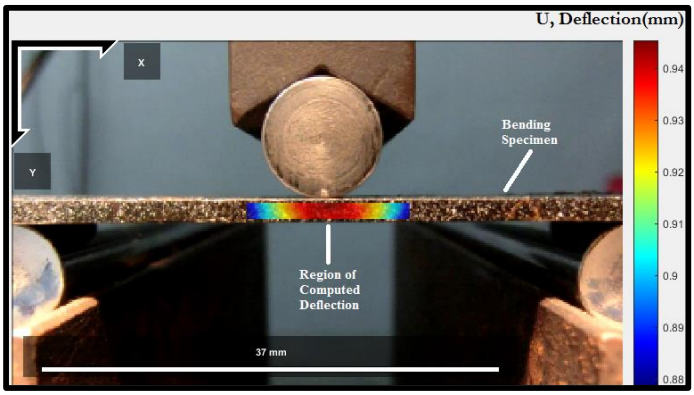

Fig. 22. Hybrid #R Deflection Computation Using DIC at 200N

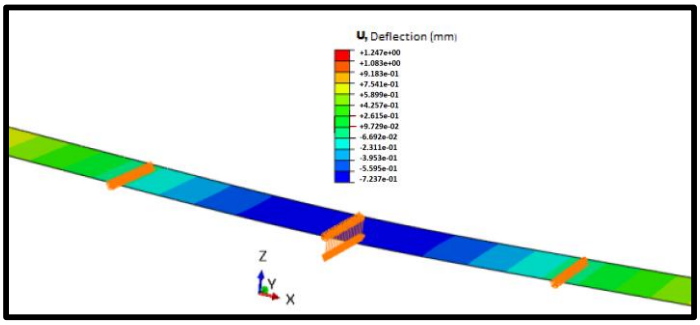

Fig. 23. Hybrid #R Deflection,U (in Z direction) Computation Using FEM at 200N

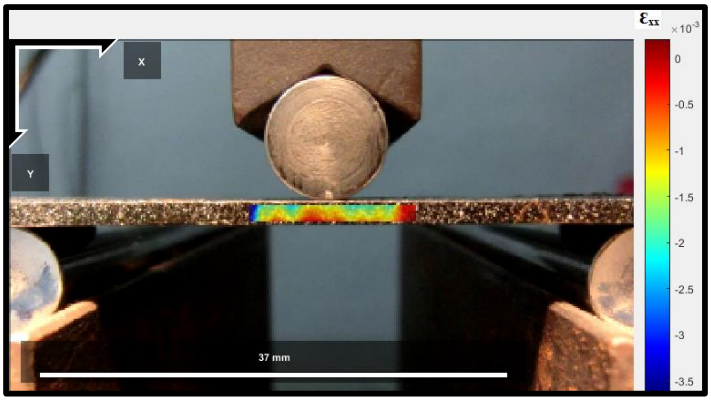

Fig. 24. Hybrid #R Strain (horizontal direction), Ɛxx using DIC at 200N

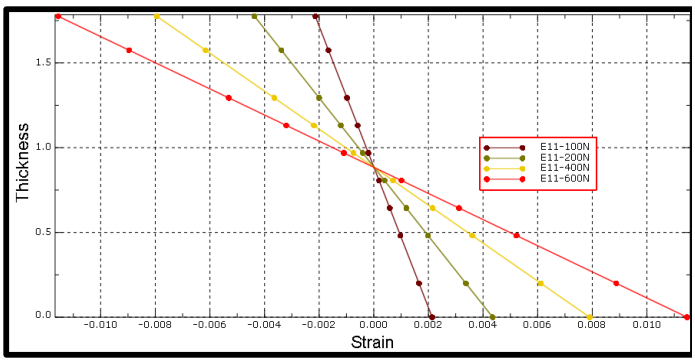

Fig. 25. Hybrid #R, Strain (horizontal), ε_{xx} Computation Using FEM at 200N

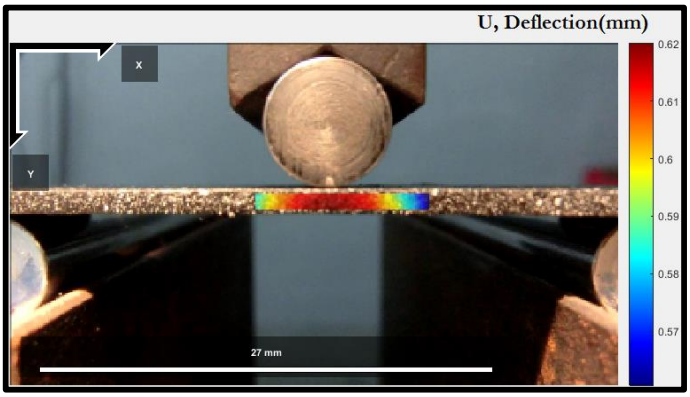

Fig. 26. Hybrid #D Deflection Computation Using DIC at 200N

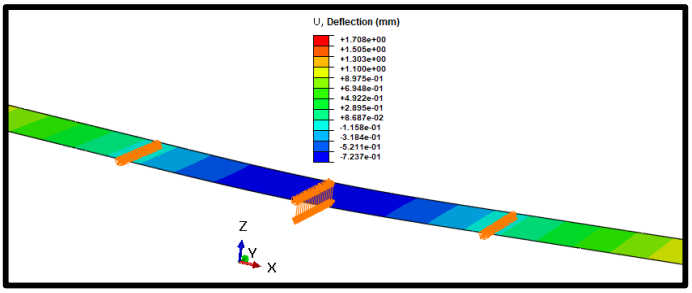

Fig. 27. Hybrid #D Deflection,U (in Z direction) Computation Using FEM at 200N

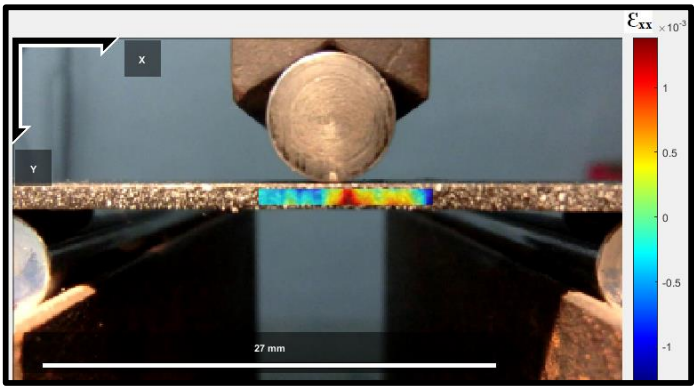

Fig. 28. Hybrid #D Strain (Horizontal Direction), ε_{xx} Computation using DIC at 200N

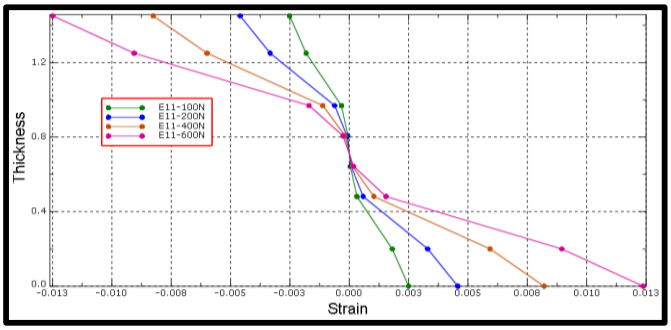

Fig. 29. Hybrid #D Strain (Horizontal Direction), ε_{xx} Computation Using FEM

Figure 30 shows the summary of the contour of DIC and FEM for horizontal strain at midsection through thickness of hybrid composite plate C/GFRP under three-point bending for Hybrid #D, Hybrid W, Hybrid#P, Hybrid #Q, and Hybrid #R. Hybrid #Q, which represents the lowest content of hybridization of GFRP into CFRP, showed the lowest deviation while Hybrid #D, which represents the highest hybrid ratio, also produces the highest deviation in terms of DIC and FEM strain measurement. Unidirectional Hybrid Composite C/GFRP (Hybrid #P, Hybrid #Q and Hybrid#R) exhibit a lower deviation as compared to Shear Dominated Hybrid Composite (Hybrid #W and Hybrid #D) due to deformation in the transverse direction which aligned with the principal fibre direction of UD Hybrid Composites. The difference between strain computed by DIC and FEM could be minimized with advanced tool such as integrated method of DIC. The strain field being a derivative was noted to be much more sensitive to noise than the displacement field. By using the integrated approach, the derivation algorithm does not generate such a short wavelength noise. It enables one to compute a displacement field which mechanically tolerable [17]. It is also possible to have the deviatation minimized if utilizing 3D DIC, which makes it possible to measure such small strain levels with a resolution proximity to 10^{-5}. Firstly, it is in reality impossible to apply on the specimen a displacement that is perfectly parallel to the CCD sensor level. Also the fact that, in the case of a perfect translation parallel to the CCD sensor plane, there will be none deformation of the subset image, which can bring to a biased computation for DIC [18].

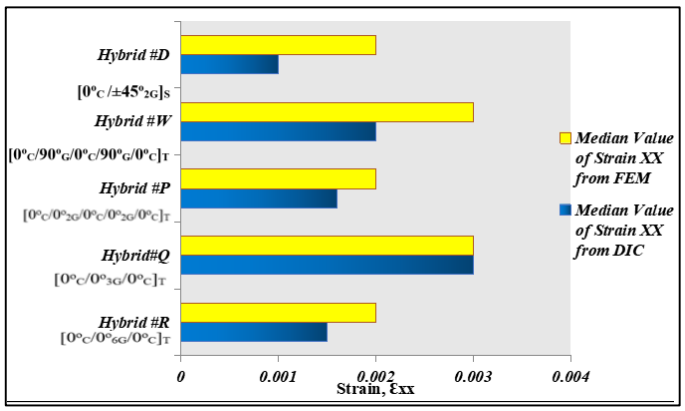

Fig. 30. Summary of Deviation of Median Value of Transverse Strain,Ɛxx of Hybrid Composites C/GFRP Under Flexural Loading at 200N

IV. Conclusion

The paper examine the in-plane full field deformation via Digital Image Correlation (DIC) on Hybrid Composite C/GFRP. Comparison of DIC on selected Hybrid Composite C/GFRP with respect to its contour of Ɛyy obtained from DIC (experimental tensile test) with FEM strain contour of Ɛyy. Comparison of DIC on Hybrid Composite C/GFRP with respect to its contour of ε_{xx} obtained from DIC (experimental) with comparison to FEM strain contour of ε_{xx} (through thickness mid plane) and deflection measurement. Full field measurement technique, digital image correlation (DIC) has been utilized to assess the deformation on tensile and flexural coupon of hybrid composite C/GFRP and comparison with FEM simulation on in plane strain has been accomplished. The comparison yielded the conclusion that deviation of median value of strain depending on the hybridization of C/GFRP where higher content of CFRP reduces the variation of strain computed from DIC on comparison with FEM simulation.

Acknowledgment

Author would like to send gratitude to Universiti Teknikal Malaysia Melaka (UTeM) for financial assistance and Faculty of Mechanical Engineering, UTeM for utilization of high speed camera, Olympus iSpeed 2. Author would also like to express special appreciation to Faculty of Mechanical Engineering, Universiti Teknologi MARA (UiTM) Shah Alam for the use of commercial software and technical expertise in composite mechanics.

References

[1] Y. Swolfs, "Perspective for fibre-hybrid composites in wind energy applications," Materials (Basel)., vol. 10, no. 11, 2017.

[2] M. M. Davoodi, S. M. Sapuan, D. Ahmad, A. Aidy, A. Khalina, and M. Jonoobi, "Concept selection of car bumper beam with developed hybrid bio-composite material," Mater. Des., vol. 32, no. 10, pp. 4857–4865, 2011.

[3] M. R. Mansor, S. M. Sapuan, E. S. Zainudin, A. A. Nuraini, and A. Hambali, "Hybrid natural and glass fibers reinforced polymer composites material selection using Analytical Hierarchy Process for automotive brake lever design," Mater. Des., vol. 51, pp. 484–492, 2013.

[4] Y. Swolfs, R. M. Mcmeeking, V. P. Rajan, F. W. Zok, and I. Verpoest, "Global load-sharing model for unidirectional hybrid fibre- reinforced composites", Journal of the Mechanics and Physics of Solids, vol. 84, pp. 380–394, 2015.

[5] G. Kretsis, "A Review of the Tensile, Compressive, Flexural and Shear Properties of Hybrid Fibre-Reinforced Plastics," Composites, vol. 18, no. 1, 1987, pp. 13–23, 1987.

[6] R. Harilal, C. P. Vyasarayani, and M. Ramji, "A linear least squares approach for evaluation of crack tip stress field parameters using DIC," Opt. Lasers Eng., vol. 75, pp. 95–102, 2015.

[7] Stepan V. Lomov, Philippe Boisse, Emmanuel de Luycker, Fabrice Morestin, Kristof Vanclooster, "Full-field strain measurements in textile deformability studies", Composites Part A: Applied Science and Manufacturing, Elsevier, vol 39, no 8, pp.1232-1244, 2008

[8] C.-C. Ho, Y.-J. Chang, J.-C. Hsu, C.-L. Kuo, S.-K. Kuo, and G.-H. Lee, "Residual Strain Measurement Using Wire EDM and DIC in Aluminum," Inventions, vol. 1, no. 1, pp 1-12, 2016.

[9] R. Harilal and M. Ramji, "Adaptation of Open Source 2D DIC Software Ncorr for Solid Mechanics Applications," 9th Int. Symp. Adv. Sci. Technol. Exp. Mech., 2014.

[10] J. Blaber, B. S. Adair, and A. Antoniou, "A methodology for high resolution digital image correlation in high temperature experiments," Rev. Sci. Instrum., vol. 86, no. 3,2015.

[11] J. Blaber, B. Adair, and A. Antoniou, "Ncorr: Open-Source 2D Digital Image Correlation Matlab Software," Exp. Mech., vol. 55, no. 6, pp. 1105–1122, 2015.

[12] P. L. Reu, W. Sweatt, T. Miller, and D. Fleming, "Camera System Resolution and its Influence on Digital Image Correlation," Exp. Mech., vol. 55, no. 1, pp. 9–25, 2015

[13] M. Z. Siddiqui, F. Tariq, and N. Naz, "Application of a Two Step Digital Image Correlation Algorithm in Determining Poisson's Ratio of Metals and Composites," 62nd Int. Astronaut. Congr., vol. 62. 2011.

[14] C.-S. T. Sze-Wei Khoo, Saravanan Karuppanan, "A review of surface deformation and strain measurement using two-dimensional digital image correlation", Metrol. Meas. Syst., vol. 23, no. 4, pp. 537–547, 2016.

[15] B. Pan, H. Xie, Z. Wang, K. Qian, and Z. Wang, "Study on subset size selection in digital image correlation for speckle patterns," Opt. Express, vol. 16, no. 10, pp 7037–7048, 2008.

[16] M. Tekieli, S. De Santis, G. de Felice, A. Kwiecień, and F. Roscini, "Application of Digital Image Correlation to composite reinforcements testing," Compos. Struct., vol 160, pp 670-688, 2017.

[17] H. F. and R. S., "Digital Image Correlation: from Displacement Measurement to Identification of Elastic Properties – a Review," Strain, vol. 42, pp. 69–80, 2006.

[18] L. Robert, F. Nazaret, T. Cutard, L. Robert, F. Nazaret, and T. Cutard, "Use of 3-D Digital Image Correlation to Characterize the Mechanical Behavior of a Fiber Reinforced Refractory Castable", Exp Mechs, vol. 47, no. 6, pp 761–773, 2007